JACS
JOURNAL OF THE AMERICAN CHEMICAL SOCIETY
Communication
pubs.acs.org/JACS

# Solution Processable MOF Yellow Phosphor with Exceptionally High Quantum Efficiency

Qihan Gong,[†] Zhichao Hu,[†] Benjamin J. Deibert,[†] Thomas J. Emge,[†] Simon J. Teat,[‡] Debasis Banerjee,[†] Brianna Mussman,[†] Nathan D. Rudd,[†] and Jing Li*[,†]

[†]Department of Chemistry and Chemical Biology, Rutgers University, 610 Taylor Road, Piscataway, New Jersey 08854, United States
[‡]Advanced Light Source, Lawrence Berkeley National Laboratory, Berkeley California 94720, United States

Supporting Information

**ABSTRACT:** An important aspect in the research and development of white light-emitting diodes (WLEDs) is the discovery of highly efficient phosphors free of rare-earth (RE) elements. Herein we report the design and synthesis of a new type of RE-free, blue-excitable yellow phosphor, obtained by combining a strongly emissive molecular fluorophore with a bandgap modulating co-ligand, in a three-dimensional metal organic framework. $[Zn_6(btc)_4(tppe)_2(DMA)_2]$ (btc = benzene-1,3,5-tricarboxylate, tppe = 1,1,2,2-tetrakis(4-(pyridin-4-yl)phenyl)-ethene, DMA = dimethylacetamide) crystallizes in a new structure type and emits bright yellow light when excited by a blue light source. It possesses the highest internal quantum yield among all RE-free, blue-excitable yellow phosphors reported to date, with a value as high as 90.7% ($\lambda_{ex}$ = 400 nm). In addition to its high internal quantum yield, the new yellow phosphor also demonstrates high external quantum yield, luminescent and moisture stability, solution processability, and color tunability, making it a promising material for use in phosphor conversion WLEDs.

Today, white light-emitting diodes (WLEDs) are gradually replacing incandescent and fluorescent lamps as a result of their lower energy consumptions, higher efficiencies, and longer lifetimes. Common approaches to fabricate WLEDs include: (a) multichip combination, where three primary colored LED chips, namely red, green, and blue (RGB) diodes are used to generate white light,[1] and (b) phosphor conversion (PC), in which white light is produced from the combined emissions of a phosphor coated on and excited by an LED chip. The combinations can be either a yellow-emitting phosphor on a blue LED chip,[2,3] a multicomponent phosphor (e.g., mixture of red-, green-, and blue-emitting material) on a UV (or near UV) chip,[4] or a white-emitting phosphor on a UV chip.[5,6] Most commercially available WLED products are PC-, rather than RGB-based, as the latter type is far more expensive. Among various PC-LEDs, both RGB and white phosphors require the use of a UV chip, which is associated with certain drawbacks, such as lower theoretical efficacy compared to blue chip WLEDs, higher input energy and cost, and possible leak of UV radiation.[7] WLEDs made of a blue chip coupled with yellow phosphor are preferred for their apparent advantages, when considering these factors,[7,8] but the disadvantage is their relatively low color rendering index (CRI) and high correlated color temperature (CCT) as a result of deficiency in red emission.[9] At the present time, almost all commercial phosphors are rare-earth (RE)-doped oxides, sulfides, oxysulfides, oxynitrides or nitrides; the RE metals, such as europium, terbium, and yttrium, are essential ingredients in these phosphors and play a crucial role in controlling their light color and quality.[3,10−13] However, as the demand of RE elements continues to increase in almost all high-tech applications, their potential supply risks and sharply raised prices (an increase of 4−49 fold from 2001 to 2011) have pushed the search for alternative RE-free phosphors to a level of high importance.[14]

Metal organic frameworks (MOFs) have attracted tremendous attention due to their potential in various applications.[15−20] The first RE-free, white-emitting MOF phosphor was reported in 2009,[21] followed by several subsequent studies on various MOFs,[22−25] however all of these materials suffer from low internal quantum yields (IQY, defined as the ratio of the number of photons emitted to the number of photons absorbed), typically <20%. Other noteworthy examples include $Eu^{2+}$- and $Eu^{3+}$-doped yellow-emitting homoleptic imidazolates[26] and white-emitting [La(mbdc)(stp)] (mbdc = isophthalate, stp = 4-(2,2′:6′,2″-terpyridin-4′-yl)benzenesulfonate)[27] as well as several LnMOFs that emit white light,[28−31] but all contain RE elements and must be excited by UV or near-UV light.

Here we report the design and synthesis of a new RE-free yellow phosphor made of MOF, $[Zn_6(btc)_4(tppe)_2(sol)_2]$. The compound emits intrinsic yellow light upon excitation with blue light with exceptionally high quantum efficiency. Recent studies by us and others reveal that emission of luminescent MOFs (LMOFs) comprised of Group 12 metals (e.g., Zn) and fluorescent ligands typically involves ligand-based electron transfer or ligand-to-ligand charge transfer (LLCT) processes.[32−34] The LMOFs often show significantly enhanced photoluminescence (PL) with respect to the constituting ligands themselves,[33,35,36] and the shift in emission energy (if any) is usually <15 nm compared to that of the ligand.[34,37,38] In order to obtain highly efficient RE-free, blue-excitable yellow phosphors, our strategy is to construct zinc-based LMOFs using highly emissive fluorophore ligands, such as tppe (1,1,2,2-tetrakis(4-(pyridin-4-yl)phenyl)ethane, Figure 1A). At room temperature, tppe emits strong green light (500 nm) with a relatively high IQY (57.2%, $\lambda_{ex}$ = 400 nm),[39] making it a suitable linker candidate.

**Received:** September 16, 2014
**Published:** November 11, 2014

 © 2014 American Chemical Society  dx.doi.org/10.1021/ja509446h | J. Am. Chem. Soc. 2014, 136, 16724−16727

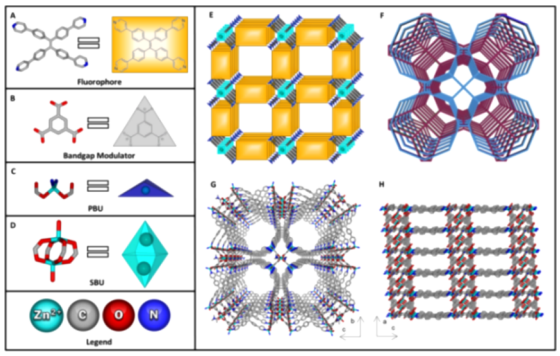


**Figure 1.** The (A) tppe and (B) btc ligands. (C) Primary and (D) secondary building units. (E) Polyhedron drawing illustrating overall connectivity. (F) Topological net of **1**. (G) 1D channels in the framework viewed along the *a*-axis. (H) Framework viewed along the *b*-axis.

However, to achieve yellow emission, a decrease in the HOMO−LUMO gap (also referred to as "bandgap" when emphasizing the nature of the infinite network of the MOFs, as an analogue of pure inorganic compounds) of the resulting LMOF with respect to that of tppe is required. We have accomplished this through a bandgap modulation approach, using 1,3,5-benzentricarboxylate (btc, Figure 1B) as a co-ligand. Our theoretical calculations employing density functional theory (DFT, see Supporting Information, S5) indicate that btc has a LUMO energy that is lower than that of tppe. This will most likely result in a reduced band gap of the LMOF built on the two ligands (Figure 2A).

Solvothermal reactions of $Zn(NO_3)\cdot 6H_2O$, tppe, and btc in dimethylacetamide (DMA) produced needle-shaped yellow crystals (70% yield). The compound crystallizes in the triclinic crystal system, space group *P-1* (Table S1), and has the general formula $[Zn_6(btc)_4(tppe)_2\ (DMA)_2]\cdot 9DMA\cdot 12H_2O$(**1**).[40] The structure is a new type of three-dimensional (3D) network with 2-fold interpenetration. The framework is built on two different building units: a primary building unit (PBU, Figure 1C), and a paddle-wheel-based secondary building unit (SBU, Figure 1D). The PBU is comprised of a tetrahedrally coordinated $Zn^{2+}$, connected to two nitrogen atoms (from two different tppe ligands) and two oxygen atoms (from two carboxylate groups of two different btc ligands); the distance of $Zn^{2+}$ to the other uncoordinated oxygen atoms that share the carboxylates is 2.6 and 2.7 Å, which is too long to be considered as bonds when compared to typical Zn−O bond lengths (~2.0 Å) found in MOFs.[41,42] The two $Zn^{2+}$ atoms in the SBU each bond to four carboxylate oxygen atoms from four different btc linkers and an oxygen atom from a DMA molecule. The two types of building units are connected by btc linkers, forming a 3D net (Figure 1E), and two such identical nets interpenetrate to give rise to the overall 3D framework (Figure 1F). The framework possesses a 1D channel along the *a*-axis (Figure 1G) with a cross section of 6.5 × 6.6 $Å^2$, measured as the closest distance between the two carbons on opposite sides of the internal wall, excluding van der Waals radius. Viewed along the *b* axis, the organic linker tppe is stacked along crystallographic (*bc*) plane (Figure 1H). The total solvent accessible volume after removal of the guest molecules is 3886.7 $Å^3$ per unit cell, or 44.1% as calculated by Platon, from which a pore volume of 0.437 $cm^3/g$ is calculated.[43] The DMA molecules act as both the terminal ligands (coordinated to the metal centers of the SBU) and as guest molecules. $H_2O$ molecules act as guest molecules and are hydrogen bonded to the carboxylate groups that are not coordinated to Zn and to each other. The point symbol of the framework is {6^2.8^4}2{6^2.8}-4{6^4.8^2}5, with a 4-nodal net topology.

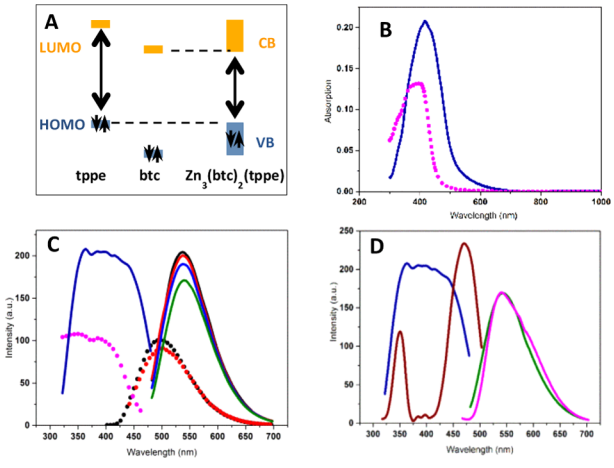


**Figure 2.** Optical properties of **1a** compared to tppe and YAG:$Ce^{3+}$. (A) Schematic presentation of orbital energies for tppe (left), btc (middle), and **1a** (right) calculated by DFT method. (B) Optical absorption spectra of tppe (dotted line, pink) and **1a** (solid line, navy blue). (C) Optical excitation (left) and emission (right) spectra of tppe and **1a**. Excitation: tppe (dotted line, pink) and **1a** (solid line, navy blue) monitored at 500 and 540 nm, respectively. Emission: tppe (dotted lines, black and red, excited at 360 and 400 nm, respectively); **1a** (solid lines, black, red, blue, and green, excited at 360, 400, 420, and 440 nm, respectively). (D) Optical excitation (left) and emission (right) spectra of **1a** and YAG:$Ce^{3+}$ (type 9800, Global Tungsten & Powders Corp.). Excitation: **1a** (navy blue) and YAG:$Ce^{3+}$ (dark red), monitored at 540 nm. Emission: **1a** (green) and YAG:$Ce^{3+}$ (pink) excited at 440 nm.

Upon standing in air for a period of time (a few days), **1** was slowly converted to **1a**, in which most or all DMA molecules are replaced by water, as confirmed by the single crystal data and elemental analysis (see SI, Sections S1, S4). The optical absorption and PL excitation and emission spectra of powder samples of both tppe and **1a** were measured at room temperature (Figure 2B,C). The estimated HOMO−LUMO and VB−CB (VB: valence band, CB: conduction band) energy gaps of tppe and **1a** are ~2.69 and ~2.38 eV, respectively, based on their optical absorption spectra collected at room temperature (Figure 2B). The decrease in the bandgap of **1a** is a result of btc modulation and is consistent with the orbital energies obtained by DFT calculations performed on the individual ligands (tppe and btc) and a fragment of MOF (Figures 2A and S5). These values are also in full accordance with their emission energies. The free tppe ligand emits green light (500 nm) when excited at 360−400 nm, which is due to intramolecular $\pi-\pi^*$ transitions, while free $H_3$btc does not emit in visible region. Upon excitation at the same wavelength (400 nm), compound **1a** emits yellow light with an emission maximum at ~540 nm and an IQY of 90.7%, a significant increase compared to 57.2% for free tppe (Table 1). To the best of our knowledge, this value is the highest among all RE-free and blue-excitable yellow phosphors reported to date. While the highest emission intensity of **1a** is achieved at an excitation wavelength of 350 nm (monitored at $\lambda_{em}$ = 540 nm, Figure 2C), it is worth noting that the excitation intensity is relatively flat from its max to ~450 nm, indicating the material can be excited effectively by a range of light sources, including blue light. Indeed, the IQY obtained at excitation wavelengths deeper into the visible region is 72.9, 67.9 and 63.9%, at 420, 440, and 450 nm, respectively. The large emission red-shift of **1a**


dx.doi.org/10.1021/ja509446h | J. Am. Chem. Soc. 2014, 136, 16724−16727

**Table 1. Quantum Yield Values of tppe and Compound 1a at Various Conditions**

| IQY (%) | | | | | |
|---|---|---|---|---|---|
| sample | $\lambda_{ex}$ = 400 nm | $\lambda_{ex}$ = 420 nm | $\lambda_{ex}$ = 440 nm | $\lambda_{ex}$ = 450 nm | $\lambda_{em}$ (nm) |
| tppe | 57.2 ± 0.6 | 40.2 ± 1.0 | 33.2 ± 1.1 | 32.1 ± 1.3 | 500 |
| **1a** | 90.7 ± 0.7 | 72.9 ± 0.5 | 67.9 ± 0.6 | 63.9 ± 0.2 | 540 |
| **TF@1a**[a] | 88.8 ± 0.6 | – | 65.3 ± 0.2 | 62.6 ± 0.1 | 540 |
| **TF@1a**[b] | 86.8 ± 0.6 | – | 63.4 ± 1.0 | 60.4 ± 0.2 | 540 |

| EQY (expressed as % of IQY, %) | | | | | |
|---|---|---|---|---|---|
| sample | $\lambda_{ex}$ = 400 nm | $\lambda_{ex}$ = 415 nm | $\lambda_{ex}$ = 440 nm | $\lambda_{ex}$ = 455 nm | $\lambda_{em}$ (nm) |
| **1a** | 96.0 | 95.3 | 91.4 | 84.7 | 540 |

| temperature-dependent PL[c] (decrease in intensity, ± 1.0%) | | | | | | | |
|---|---|---|---|---|---|---|---|
| sample | 80 °C | 100 °C | 120 °C | 140 °C | 150 °C | 160 °C | $\lambda_{em}$ (nm) |
| **TF@1a** ($\lambda_{ex}$ = 440 nm) | 0.0 | 0.0 | 0.0 | −3.0 | −3.5 | −6.0 | 540 |

[a]Teflon protected sample after being heated at 120 °C for 12 h and subsequently cooled to room temperature. [b]Teflon protected sample after being heated at 150 °C for 12 h and subsequently cooled to room temperature. [c]After being heated at indicated temperature for 12 h and subsequently cooled to room temperature.

compared to tppe is a result of incorporating btc as a bandgap modulator, which leads to a decrease in the bandgap energy and corresponding emission (Figures 2A,C and S5 and Table S2). Based on a number of recent reports on similar MOF systems, the strong PL enhancement of **1a** can be attributed to the immobilization of tppe in the MOF backbone which effectively reduces nonradiative decay due to molecular vibration and rotation.[36,44,45] The external QYs (EQY, defined as the ratio of the number of photons emitted to the number of incident photons) of **1a** were measured on a QE2000 system (see SI for details) and are listed in Table 1. At 400, 415, 440, and 455 nm, they account for 96%, 95.3%, 91.4% and 84.7% of the IQY values, respectively, indicating high absorption efficiency of the compound (nearly 100%).

A comparison between **1a** and a commercial yellow phosphor, cerium-doped yttrium aluminum garnet (YAG:$Ce^{3+}$) revealed remarkable similarity in emission properties (Figures 2D, S6, and S7). The Commission International de l'Eclairage coordinates of **1a** (0.39, 0.57) are well within the yellow range and are very close to those of YAG:$Ce^{3+}$ (0.41, 0.56) (Figure S6). The emission spectra of the two are nearly identical (Figure 2D) at room temperature. The dispersible nature of compound **1a** in selected solutions makes it possible to coat the samples on flexible substrates, such as a rope or thin cotton strings, which is not possible with traditional inorganic yellow phosphors such as YAG:$Ce^{3+}$. We demonstrate this in Figure 3, where dispersed samples of **1a** were coated on thin cotton strings and then illuminated under a 12 W blue LED lamp (emission range: 450−470 nm, ABI LED Lighting Company); Figure 3A,C shows coated/uncoated strings under daylight, and Figure 3B,D shows the same string under the blue light.

A prototype WLED device was assembled using a 5 mm 455−460 nm blue LED bulb, with sample **1a** coated on the surface (Figure 3E). The coating solution was prepared by dispersing powders of **1a** in ethyl acetate under ultrasonication for 1 h. The blue LED bulb was then dipped into the suspension solution several times until a thin and uniform film formed on the surface

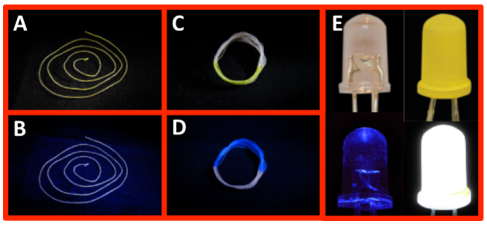


**Figure 3.** (A−E) Images of dispersed sample **1a** coated on thin cotton strings and LED bulb. Top row: images of samples under daylight. Bottom row: images of samples illuminated by a 450 nm blue LED. (A,B) **1a** coated on a single cotton string. (C,D) A wound-up string with the bottom half coated with **1a** and the top half uncoated. (E) WLED assembly. Left half: blue LED bulb before (top) and after (bottom) being illuminated. Right half: the same blue LED coated by a dispersed sample of **1a** before (top) and after (bottom) being illuminated.

of the bulb; bright white light was generated when a 3 V bias was applied. The luminous efficacy of the WLED device was measured to be 47.4 lm/W, well above the requirement of commercial LED lamps (e.g., the minimum requirement for small LED directional lamps 40 lm/W)[46] and can doubtlessly be improved upon, as the device was not optimized for performance.

To further verify the suitability of the material for potential use in PC-WLEDs, stability measurements were carried out on **1a** and an assembly of **1a** with Teflon film (**TF@1a**, see Figure S8). Compound **1a** exhibits high moisture stability at room temperature; a sample of **1a** was left sitting in air for a period >3 months, after which time a PXRD measurement verified the material's structural integrity (Figure S10). At excitation wavelength of 455 nm, the IQY of **1a** was measured as 58.1% originally, and 57.6% after being exposed to air for 3 months, with <1% decrease over this long period of time. Only a small decrease in the emission intensity was observed upon continuous irradiation of the sample under a UV lamp (365 nm) for 7 days (Figure S12). The thermal stability of **1a** and **TF@1a** was examined at various temperatures. Thermogravimetric analysis (Figure S9) shows that **1a** undergoes continuous weight loss from room temperature to ∼220 °C, then remains stable until ∼300 °C, at which point the framework starts to decompose. PXRD and PL data were collected after **TF@1a** was heated at different temperatures for a given period of time (e.g., 12 h), which show the material is both thermally and optically stable up to 180 °C (Figure S11). Decreases in PL intensity and IQY are <3.5% and 6.7%, respectively, upon heating at 150 °C for 12 h (Table 1).

Solvent exchange of **1a** was carried out at room temperature by soaking freshly as-made sample in various solvents for 2 days (replacing once with fresh solvent), followed by PXRD structural verification (Figure S13). PL emission spectra of the exchanged samples show shifted emission wavelengths and varying intensities (Figure S14).

In summary, we have designed and synthesized a new type of yellow phosphor totally free of RE elements. This was achieved by combining a highly emissive molecular fluorophore with a bandgap regulating co-ligand into a MOF structure, thus tuning the HOMO−LUMO energy gap to attain desired excitation and emission properties. The new yellow phosphor can be effectively excited by a blue LED chip and assembled in a PC-WLED. Compound **1a** and selected solvent exchanged samples (**1a**·sol) exhibit significantly enhanced emission compared to the constituent ligand (tppe). To the best of our knowledge, the


dx.doi.org/10.1021/ja509446h | J. Am. Chem. Soc. 2014, 136, 16724−16727

RT IQY of compound **1a** (90.7% at $\lambda_{ex}$ = 400 nm) is the highest among all yellow emitting MOFs reported to date. In addition, the high solution processability of this compound enables its utility in flexible light fixtures. The exceptionally high performance of **1a** and **1a**·sol makes them promising candidates for use as an alternate yellow phosphor in PC-WLEDs. The structure design and bandgap modulation approach can be generalized and applied to many other metal/ligand combinations.

## ■ ASSOCIATED CONTENT

### Supporting Information

Experimental data and characterization data. Crystallographic data for the reported crystal structures have been deposited at the Cambridge Crystallographic Data Centre via www.ccdc.cam.ac.uk with code 993904. This material is available free of charge via the Internet at http://pubs.acs.org.

## ■ AUTHOR INFORMATION


### Corresponding Author

jingli@rutgers.edu


### Notes

The authors declare no competing financial interest.

## ■ ACKNOWLEDGMENTS

The authors acknowledge the National Science Foundation for the financial support (grant no. DMR-1206700). The Advanced Light Source (ALS) is supported by the Director, Office of Science, Office of Basic Energy Sciences, of the U.S. Department of Energy under contract no. DE-AC02-05CH11231. Q.G. would like to specially thank Dr. Jingming Zhang and Dr. Sujing Wang for their help in improving the ligand synthesis method.

## ■ REFERENCES


(1) Muthu, S.; Schuurmans, F. J. P.; Pashley, M. D. *IEEE J. Sel. Top. Quantum Electron.* **2002**, *8*, 333.

(2) Jang, H. S.; Jeon, D. Y. *Appl. Phys. Lett.* **2007**, *90*, 041906.

(3) Xie, R. J.; Hirosaki, N.; Sakuma, K.; Yamamoto, Y.; Mitomo, M. *Appl. Phys. Lett.* **2004**, *84*, 5404.

(4) Sheu, J. K.; Chang, S. J.; Kuo, C. H.; Su, Y. K.; Wu, L. W.; Lin, Y. C.; Lai, W. C.; Tsai, J. M.; Chi, G. C.; Wu, R. K. *IEEE Photonics Technol. Lett.* **2003**, *15*, 18.

(5) Dohner, E. R.; Hoke, E. T.; Karunadasa, H. I. *J. Am. Chem. Soc.* **2014**, *136*, 1718.

(6) Roushan, M.; Zhang, X.; Li, J. *Angew. Chem., Int. Ed.* **2012**, *51*, 436.

(7) Pimputkar, S.; Speck, J. S.; DenBaars, S. P.; Nakamura, S. *Nat. Photonics* **2009**, *3*, 180.

(8) Allen, S. C.; Steckl, A. J. *Appl. Phys. Lett.* **2008**, *92*, 143309.

(9) Daicho, H.; Iwasaki, T.; Enomoto, K.; Sasaki, Y.; Maeno, Y.; Shinomiya, Y.; Aoyagi, S.; Nishibori, E.; Sakata, M.; Sawa, H.; Matsuishi, S.; Hosono, H. *Nat. Commun.* **2012**, *3*, 1132.

(10) Hoppe, H. A. *Angew. Chem., Int. Ed.* **2009**, *48*, 3572.

(11) Im, W. B.; Kim, Y. I.; Fellows, N. N.; Masui, H.; Hirata, G. A.; DenBaars, S. P.; Seshadri, R. *Appl. Phys. Lett.* **2008**, *93*, 091905.

(12) Song, Y. H.; Jia, G.; Yang, M.; Huang, Y. J.; You, H. P.; Zhang, H. J. *Appl. Phys. Lett.* **2009**, *94*, 091902.

(13) Im, W. B.; Brinkley, S.; Hu, J.; Mikhailovsky, A.; DenBaars, S. P.; Seshadri, R. *Chem. Mater.* **2010**, *22*, 2842.

(14) Bauer, D.; Diamond, D.; Li, J.; McKittrick, M.; Sandalow, D.; Telleen, P. *Critical Materials Strategy*; U.S. DOE: Washington, DC, 2011.

(15) Cui, Y. J.; Yue, Y. F.; Qian, G. D.; Chen, B. L. *Chem. Rev.* **2012**, *112*, 1126.

(16) Li, J. R.; Sculley, J.; Zhou, H. C. *Chem. Rev.* **2012**, *112*, 869.

(17) Yoon, M.; Srirambalaji, R.; Kim, K. *Chem. Rev.* **2012**, *112*, 1196.

(18) Hu, Z.; Deibert, B. J.; Li, J. *Chem. Soc. Rev.* **2014**, *43*, 5815.

(19) Perry, J. J.; Perman, J. A.; Zaworotko, M. J. *Chem. Soc. Rev.* **2009**, *38*, 1400.

(20) Li, M.; Li, D.; O'Keeffe, M.; Yaghi, O. M. *Chem. Rev.* **2014**, *114*, 1342.

(21) Wang, M. S.; Guo, S. P.; Li, Y.; Cai, L. Z.; Zou, J. P.; Xu, G.; Zhou, W. W.; Zheng, F. K.; Guo, G. C. *J. Am. Chem. Soc.* **2009**, *131*, 13572.

(22) He, J.; Zeller, M.; Hunter, A. D.; Xu, Z. T. *J. Am. Chem. Soc.* **2012**, *134*, 1553.

(23) Sava, D. F.; Rohwer, L. E. S.; Rodriguez, M. A.; Nenoff, T. M. *J. Am. Chem. Soc.* **2012**, *134*, 3983.

(24) Sun, C. Y.; Wang, X. L.; Zhang, X.; Qin, C.; Li, P.; Su, Z. M.; Zhu, D. X.; Shan, G. G.; Shao, K. Z.; Wu, H.; Li, J. *Nat. Commun.* **2013**, *4*, 2717.

(25) Luo, F.; Wang, M. S.; Luo, M. B.; Sun, G. M.; Song, Y. M.; Li, P. X.; Guo, G. C. *Chem. Commun.* **2012**, *48*, 5989.

(26) Rybak, J. C.; Hailmann, M.; Matthes, P. R.; Zurawski, A.; Nitsch, J.; Steffen, A.; Heck, J. G.; Feldmann, C.; Gotzendorfer, S.; Meinhardt, J.; Sextl, G.; Kohlmann, H.; Sedlmaier, S. J.; Schnick, W.; Muller-Buschbaum, K. *J. Am. Chem. Soc.* **2013**, *135*, 6896.

(27) Wei, Y. Q.; Li, Q. H.; Sa, R. J.; Wu, K. C. *Chem. Commun.* **2014**, *50*, 1820.

(28) Zhang, X. J.; Ballem, M. A.; Hu, Z. J.; Bergman, P.; Uvdal, K. *Angew. Chem., Int. Ed.* **2011**, *50*, 5729.

(29) Sava Gallis, D. F.; Rohwer, L. E. S.; Rodriguez, M. A.; Nenoff, T. M. *Chem. Mater.* **2014**, *26*, 2943.

(30) Liu, Y.; Pan, M.; Yang, Q. Y.; Fu, L.; Li, K.; Wei, S. C.; Su, C. Y. *Chem. Mater.* **2012**, *24*, 1954.

(31) Dang, S.; Zhang, J. H.; Sun, Z. M. *J. Mater. Chem.* **2012**, *22*, 8868.

(32) Pramanik, S.; Zheng, C.; Zhang, X.; Emge, T. J.; Li, J. *J. Am. Chem. Soc.* **2011**, *133*, 4153.

(33) Li, X.; Wang, X. W.; Zhang, Y. H. *Inorg. Chem. Commun.* **2008**, *11*, 832.

(34) Guo, H. D.; Guo, X. M.; Batten, S. R.; Song, J. F.; Song, S. Y.; Dang, S.; Zheng, G. L.; Tang, J. K.; Zhang, H. J. *Cryst. Growth Des.* **2009**, *9*, 1394.

(35) Hu, Z.; Pramanik, S.; Tan, K.; Zheng, C.; Liu, W.; Zhang, X.; Chabal, Y. J.; Li, J. *Cryst. Growth Des.* **2013**, *13*, 4204.

(36) Lin, J. G.; Xu, Y. Y.; Qiu, L.; Zang, S. Q.; Lu, C. S.; Duan, C. Y.; Li, Y. Z.; Gao, S.; Meng, Q. J. *Chem. Commun.* **2008**, 2659.

(37) Feng, P. L.; Perry, J. J.; Nikodemski, S.; Jacobs, B. W.; Meek, S. T.; Allendorf, M. D. *J. Am. Chem. Soc.* **2010**, *132*, 15487.

(38) Zhang, C. Y.; Che, Y. K.; Zhang, Z. X.; Yang, X. M.; Zang, L. *Chem. Commun.* **2011**, *47*, 2336.

(39) Kapadia, P. P.; Widen, J. C.; Magnus, M. A.; Swenson, D. C.; Pigge, F. C. *Tetrahedron Lett.* **2011**, *52*, 2519.

(40) Crystal data for **1**: $C_{172}H_{199}N_{19}O_{47}Zn_6$, $M$ = 3676.71 g/mol; triclinic, space group $P$-1; $a$ = 10.1093(13) Å, $b$ = 29.515(4) Å, $c$ = 29.532(4) Å, $\alpha$ = 91.444(2)°, $\beta$ = 93.316(3)°, $\gamma$ = 91.622(3)°; $V$ = 8790(2) Å$^3$; $Z$ = 2.

(41) Li, W.; Probert, M. R.; Kosa, M.; Bennett, T. D.; Thirumurugan, A.; Burwood, R. P.; Parinello, M.; Howard, J. A. K.; Cheetham, A. K. *J. Am. Chem. Soc.* **2012**, *134*, 11940.

(42) Lee, J. Y.; Pan, L.; Kelly, S. R.; Jagiello, J.; Emge, T. J.; Li, J. *Adv. Mater.* **2005**, *17*, 2703.

(43) Spek, A. L. *PLATON: A Multipurpose Crystallographic Tool*; Utrecht University: Utrecht, The Netherlands, 2001.

(44) Shustova, N. B.; McCarthy, B. D.; Dincă, M. *J. Am. Chem. Soc.* **2011**, *133*, 20126.

(45) Wei, Z. W.; Gu, Z. Y.; Arvapally, R. K.; Chen, Y. P.; McDougald, R. N.; Ivy, J. F.; Yakovenko, A. A.; Feng, D. W.; Omary, M. A.; Zhou, H. C. *J. Am. Chem. Soc.* **2014**, *136*, 8269.

(46) Pacific Northwest National Laboratory. *SSL Pricing and Efficacy Trend Analysis for Utility Program Planning*; U.S. DOE: Washington, DC, 2013.